Low energy electron microscopy of quantum well resonances in Ag films on W(110)

2005 J. Phys.: Condens. Matter 17 S1305

(http://iopscience.iop.org/0953-8984/17/16/001)

INSTITUTE OF PHYSICS PUBLISHING JOURNAL OF PHYSICS: CONDENSED MATTER

J. Phys.: Condens. Matter **17** (2005) S1305–S1310 doi:10.1088/0953-8984/17/16/001

Low energy electron microscopy of quantum well resonances in Ag films on W(110)

M S Altman

Department of Physics, Hong Kong University of Science and Technology, Clear Water Bay, Kowloon, Hong Kong

E-mail: phaltman@ust.hk

Received 9 December 2004, in final form 9 December 2004
Published 8 April 2005
Online at stacks.iop.org/JPhysCM/17/S1305

Abstract

Laterally resolved measurements of the quantum size effect in electron reflectivity are made with low energy electron microscopy on Ag films on a W(110) surface. Intensity peaks are observed that are associated with quantum well (QW) resonances above the vacuum level. The unoccupied band structure in the ΓL direction is determined from a phase accumulation model analysis of experimental data. This analysis also identifies a substantial influence of the reflection phase at the W(110) interface on the QW resonance intensity peak positions observed in experiment.

1. Introduction

The properties of ultrathin metal films exhibit remarkable quantum size effects (QSEs) due to the discrete quantum well states that are caused by electron confinement. In the ultrathin film geometry, electron confinement is imposed by the vacuum on one side and by a bandgap in the supporting substrate on the other side of film. This effectively creates a one-dimensional quantum well (QW) in the direction perpendicular to the film. Considerable attention has been given to the study of QW electronic states below the vacuum level with photoemission and inverse photoemission [1, 2]. A key observation is that the QW state binding energy varies systematically with film thickness. The dependence of QW state binding energy upon film thickness is well understood by the phase accumulation model [1, 3]. An important consequence is that QW states periodically cross the Fermi level. This has been shown to have an impact on structure, magnetism and chemical properties of thin films.

Measurements of the elastically reflected electron intensity from metallic thin films also often reveal intensity peaks at very low energy that are associated with QW resonances above the vacuum level. This QSE in electron reflectivity can be understood to be an interference phenomenon between the electron waves that are reflected from the surface of the film and from the interface between the film and substrate. Consequently, this interference periodically modulates the reflected intensity both as a function of film thickness and energy. In direct correspondence with the binding energies of QW states below vacuum, the energies of QW

resonances are very sensitive to film thickness. However, intensity peaks associated with QW resonances are weak when the inelastic mean free path is short compared to the film thickness and reflection from buried interface is weak. That is why QW resonances are not observed at energies used in conventional low energy electron diffraction (LEED), and why it is crucial to work at very low energy.

Although the QSE in electron reflectivity has been known for a long time [4, 5], it has only been exploited recently to extract detailed information on unoccupied electron band structure above the vacuum level [6] and to determine details of film structure [7, 8]. These recent advances in understanding and application of the QSE in electron reflectivity were based on measurements of electron reflectivity with low energy electron microscopy (LEEM). One advantage of this approach is that LEEM is capable of handling electrons at very low energy with minimal disturbance caused by stray fields. Laterally resolved measurements in LEEM also discriminate information from regions of different film thicknesses with atomic vertical resolution. This facilitates the comparison of experimental data to model calculations for idealized uniformly thick films.

In this paper, we use the phase accumulation model to understand the dependence of QW resonances in Ag/W(110) films on film thickness and incident electron energy. Application of this model first provides information on unoccupied band structure in the Ag film in the ΓL direction, which agrees with theoretical predictions. This analysis also reveals that a phase shift is caused by scattering at the buried W(110) interface over much of the energy range where QW resonances are observed. This phase shift has a substantial influence on the QW resonance conditions and must be understood in detail in order to accurately describe intensity peaks observed in experiment.

2. Results and discussion

It is known from earlier studies that Ag grows pseudomorphically on W(110) initially and that a strained fcc Ag(111) film structure is well developed at two monolayer (ML) thickness [8–10]. Although no significant change of in-plane film structure was detected for thickness above 2 ML in the previous work [8, 9], a detailed LEED analysis has shown that the transformation from pseudomorphic to fcc structure is not complete until the third layer is completed [11]. Ag was deposited in our experiments at a rate of 0.33 ML min^{-1} onto a sample held at about 500 K. The experiments were carried out in a LEEM with base pressure of 2×10^{-10} Torr and the measurements were made at room temperature. The imaging principle and contrast mechanisms of LEEM have been discussed previously [7, 12].

An example of a LEEM image of a Ag film on W(110) is shown in figure 1. The QSE in electron reflectivity is manifested vividly in this image as quantum size contrast between regions of different thickness. By varying the incident electron energy and measuring the intensity in uniformly thick regions, single-thickness $I(V)$ spectra are obtained simultaneously for all of the different thicknesses present in the image field of view. The $I(V)$ curves of the (00) beam at normal incidence (no parallel momentum transfer) obtained in this manner clearly show prominent intensity peaks that are associated with QW resonances (figure 2). The QW resonance conditions are the focus of the analysis that is described next.

The QW resonances that give rise to intensity peaks in electron reflectivity can be understood by applying the phase accumulation model [3]. According to this model, the quantization condition for the existence of QW states and resonances is

$$2k(E)mt + \Phi(E) = 2n\pi, \tag{1}$$

where $k(E)$ is the perpendicular wavevector of an electron in the film, m is the number of atomic layers, t is the average layer spacing, $\Phi(E)$ is the energy dependent phase shift

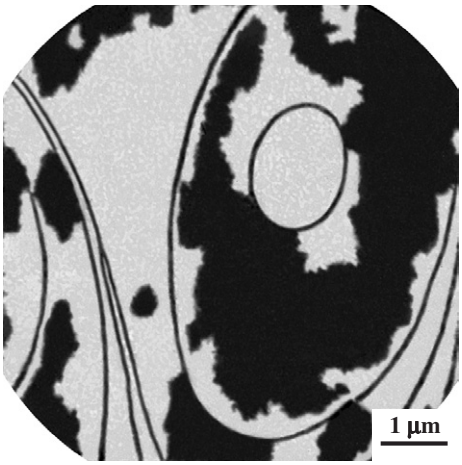

Figure 1. LEEM image of a Ag film on W(110) which shows quantum size contrast between regions of different film thickness. The imaging energy is $E = 5.8$ eV (from [8]).

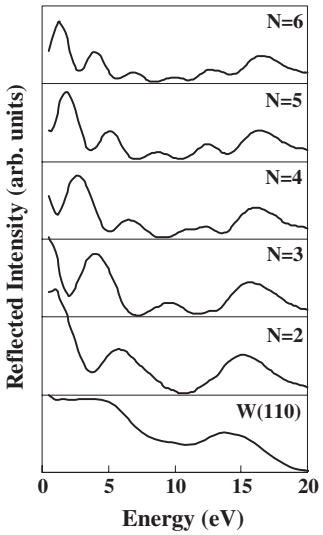

Figure 2. Quantum interference peaks in electron reflectivity for $N = 2$–6 ML Ag films on W(110). The $I(V)$ curve of the clean W(110) surface is also shown.

accumulated upon reflection at the interface and surface, and n is an integer. Intensity maxima occur in electron reflectivity when this condition is met. (The intensity minima between the intensity peaks occur when n is replaced by $(2n + 1)/2$ in equation (1).) Equation (1) can be inverted to obtain the following expression [3]:

$$m = \frac{\Phi(E)/2\pi + \nu}{\kappa(E)/k_{\mathrm{BZ}}}, \tag{2}$$

where the quantum number $\nu = m - n$ for intensity maxima ($\nu = m - n - \frac{1}{2}$ for minima), $k_{\mathrm{BZ}} = \pi/t$ and the wavevector $\kappa(E) = k_{\mathrm{BZ}} - k(E)$ is measured from the Brillouin zone boundary in the direction perpendicular to the film plane, i.e., the L point for Ag(111). The energies of the intensity maxima and minima are plotted as a function of film thickness in figure 3. The maximum and minimum points in figure 3 were determined after normalizing the raw experimental data in figure 2 by an $I(V)$ curve for a thick Ag(111) film that shows no QW resonance intensity peaks. The points for different thickness having integer quantum number ν (intensity maxima) are indicated by filled circles in figure 3. The curves that connect these points are discussed below. Open circles in figure 3 that lie between the connected filled circles indicate intensity minima with the same half integer quantum number. The dashed curves that connect these points have no physical significance.

The unknown phase $\Phi(E)$ can be eliminated by subtracting equation (2) for pairs of data points that occur at the same energy. Then, one obtains an expression $\kappa(E) = \pi(\nu_2 - \nu_1)/(m_2 - m_1)t$ for these energies. The $E(k)$ plot that is determined by applying the phase accumulation model is shown in figure 4. The two-layer film data were not included in this calculation because the strained Ag(111) structure is not fully developed. For comparison, the results of self-consistent non-relativistic band structure calculations for Ag [13] are shown, where we have assumed a work function of 4.45 eV [14]. The experimental data are in excellent agreement with the calculated dispersion. The scatter of data points about the theoretical curve gives an indication of the experimental uncertainty. It should be noted that the energy scale of the $I(V)$ curves plotted in figure 2 is referenced to the vacuum level. This level was determined

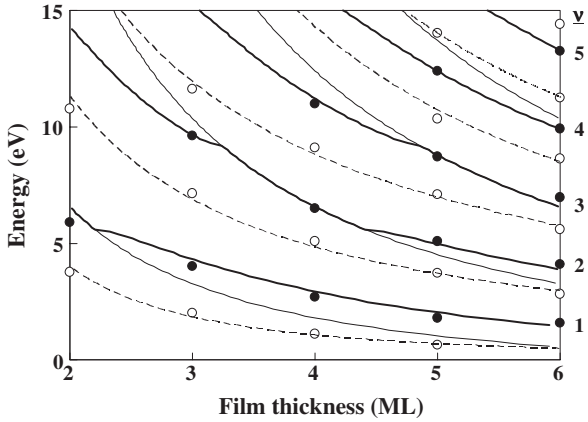

Figure 3. The energies of intensity maxima (●) and minima (○) for Ag films with thicknesses between two and six monolayers (ML). The thick solid curves that connect maxima are phase accumulation model predictions including interface reflection phase for the indicated quantum numbers ν. The thin solid curves indicate phase accumulation model predictions without the interface reflection phase. The dashed curves through the minima are meant just as a guide to the eye.

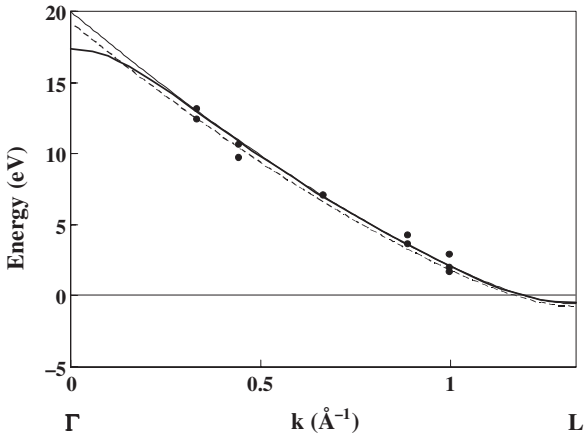

Figure 4. The $E(k)$ dispersion along the ΓL direction of Ag determined from the data in figure 3 is shown in comparison to the calculated band structure from [13] (thick solid curve). The thin solid (dashed) curve is the nearly free electron model band with $V_0 = -10.15$ eV, $U = 2.1$ eV, and $m^* = 0.90\ m_e$ ($m^* = 0.93\ m_e$). The energy scale is referenced to the vacuum level ($E_{vac} = 0$).

by the onset of perfect reflection from the surface, which was found by biasing the sample negatively with respect to the electron gun cathode by 1 V. This offset originates in the work function difference between the sample and cathode.

The energy band in figure 4 can be conveniently described by the nearly free electron model [15]. According to this model, the $\kappa(E)$ of a nearly free electron band is expressed as

$$\kappa(E) = \left(\frac{2m^*}{\hbar^2}\right)^{1/2} \left\{ G + \frac{E - V_0}{G} - \left[4\left(\frac{E - V_0}{G}\right) + \frac{U^2}{G^2} \right]^{1/2} \right\}^{1/2} \tag{3}$$

where E is the electron energy, V_0 is the mean crystal potential (a constant offset of the periodic potential), U is the pseudopotential form factor (the amplitude of the periodic potential,

equal to half of the bandgap at the zone boundary), m^* is the electron effective mass, and $G = \hbar^2 k_{BZ}^2/2m^*$. This model parametrizes the band with only three quantities. In particular, the fit to the theoretical band shown in figure 4 is obtained with $V_0 = -10.15$ eV relative to the vacuum level ($E_{vac} = 0$), $U = 2.1$ eV, and $m^* = 0.90\, m_e$, where m_e is the electron mass. The nearly free electron model band is virtually indistinguishable from the theoretical prediction of [13] over most of the Brillouin zone between $0.26\ \text{Å}^{-1} < k < k_{BZ}$. Deviation is seen (thin line in figure 4) only where we have not bothered to model the bandgap near the zone centre as we have at the zone boundary.

The nearly free electron band described by equation (3) can now be used in conjunction with equation (2) to predict the conditions for QW resonance peaks to occur according to the phase accumulation model. This is done by treating film thickness, m, as a continuous variable and solving equation (2) for different values of the quantum number, ν. To begin with, we discuss the predictions where the reflection phase, $\Phi(E)$, is disregarded. These predictions, shown as thin solid curves through the QW resonance peaks (filled circles) in figure 3, clearly miss the data at low and high energy. A substantially better set of predictions is obtained when the reflection phase is included. The strategy for treating the reflection phase is based on the principle that the phase must change by π as the energy of the incident electron traverses a bandgap. This is described by an empirical formula, which is a modified form of the phase that has been used previously to understand QW states [3]

$$\Phi(E) = s\pi - 2\arcsin\sqrt{\frac{E - E_L}{E_U - E_L}} \tag{4}$$

where E_L and E_U are the lower and upper edge of the bandgap, respectively, and s is an integer. According to theory, the relevant bandgap for W(110) exists between about $E_L = 0.6$ eV and $E_U = 5.6$ eV above the vacuum level [16, 17]. This is supported by experimental observations of a high reflected intensity in the (00) beam at normal incidence in this energy range (figure 2). Figure 2 also reveals a second intensity peak centred at about $E = 14$ eV. This is probably associated with a symmetry gap caused by band hybridization, where there are no states of the correct symmetry for plane waves to couple to from vacuum. We identify a possible symmetry gap in the calculated band structure [16, 17] that lies between $E_L = 9.2$ eV and $E_U = 15.5$ eV, which corresponds roughly with the position and the energy width of the experimental intensity peak centred at $E = 14$ eV in figure 2. The gaps at low and high energy are then incorporated into the phase accumulation model as reflection phases that vary according to equation (4) with $s = 1$ and 0, respectively. After this treatment of the reflection phase, a much better agreement between experimental data and phase accumulation model predictions is obtained. It should be noted that an effective mass of $m^* = 0.93\, m_e$ was used to generate the phase accumulation model predictions in figure 3, which is larger than the value of m^* that was determined from fitting the theoretical band in figure 4. The larger value of m^* gave a slightly better fit to the experimental QW resonance peak data in figure 3, and generated a nearly free electron band (thin dashed curve in figure 4) that was still within experimental uncertainty of the experimental $E(k)$ data points in figure 4.

It is important to note that the analysis described above has been carried out assuming that the Ag film has uniform structure from the surface to the buried interface. An interesting question concerns the possible influence of structural variations within the film on the QW resonance conditions. In particular, the deepest Ag layer may be more highly strained than the rest of the film due to its direct interaction with the W substrate. Localization of strain at the interface raises concern of misinterpretation of the substrate reflection phase. However, we expect that strain localized at the interface would shift the QW resonances from the phase accumulation model predictions excluding the reflection phase (thin curve in figure 3) in a

uniform direction over the entire energy range. The shift could be either to higher or to lower energy, depending upon whether the strain is tensile or compressive. This can be distinguished from the reflection phase encapsulated in equation (4), which occurs only in energy ranges that correspond to substrate bandgaps. This reflection phase causes QW resonances to shift above and below the phase accumulation model prediction (without the reflection phase) in the different bandgap energy ranges. Furthermore, the impact of strain localized in the Ag layer at the interface on the QW resonance conditions would diminish as the film gets thicker because the phase accumulated in traversing this layer would be a diminishing component of the total phase accumulated over the entire film. Thus, we expect that the QW resonance conditions would converge at larger thicknesses with the phase accumulation model predictions that exclude the reflection phase. There is no clear evidence that the QW resonance conditions are influenced by localized strain at the interface. The fact that the substrate reflection phase (equation (4)) works so well is an indication either that the structure of the deepest Ag layer does not differ significantly from the rest of the film or that the QW resonance conditions are insensitive to this detail of film structure.

3. Conclusions

The quantum size effect in electron reflectivity from thin films gives rise to interference peaks that are related to quantum well resonances. Laterally resolved measurements of this effect with low energy electron microscopy discriminate information from regions of different film thicknesses with atomic vertical resolution. This facilitates the analysis of unoccupied band structure above the vacuum level using the phase accumulation model. When the phase accumulation quantization rule is used to sample several k-points for strained Ag(111) films on W(110), an experimental $E(k)$ dispersion in the ΓL direction is determined that agrees with predictions of theoretical band structure calculations. However, comparison of phase accumulation model predictions to experimental data indicates that the reflection phase at the buried interface has a significant impact on the energies that QW resonance intensity peaks occur. In addition to bandgaps with no available electronic states, we find that symmetry gaps also cause reflection phases which shift QW resonance peaks. Future work on the QSE in electron reflectivity must consider these details of substrate band structure.

References

[1] Chiang T C 2000 *Surf. Sci. Rep.* **39** 181
[2] Ortega J E, Himpsel F J, Mankey G J and Willis R F 1993 *Phys. Rev.* B **47** 1540
[3] Smith N V, Brookes N B, Chang Y and Johnson P D 1994 *Phys. Rev.* B **49** 332
[4] Jonker B T, Bartelt N C and Park R L 1983 *Surf. Sci.* **127** 183
[5] Jacklevic R C 1984 *Phys. Rev.* B **30** 5494
[6] Zdyb R and Bauer E 2002 *Phys. Rev. Lett.* **88** 166403
[7] Altman M S, Chung W F and Liu C H 1998 *Surf. Rev. Lett.* **5** 1129
[8] Chung W F, Feng Y J, Poon H C, Chan C T, Tong S Y and Altman M S 2003 *Phys. Rev. Lett.* **90** 216105
[9] Bauer E *et al* 1977 *J. Appl. Phys.* **48** 3773
[10] Yang Y W, Xu H and Engel T 1992 *Surf. Sci.* **276** 341
[11] Poon H C, Chung W F, Tong S Y and Altman M S, unpublished
[12] Bauer E 1994 *Rep. Prog. Phys.* **57** 895
[13] Fuster G, Tyler J M, Brener N E, Callaway J and Bagayoko D 1990 *Phys. Rev.* B **42** 7322
[14] Jakobi K 1994 *Physics of Solid Surfaces* (*Landolt–Börnstein, New Series* Group III, vol 24, pt. b) ed G Chiarotti (Berlin: Springer) p 63
[15] Ashcroft N W and David Mermin N 1976 *Solid State Physics* (Philadelphia, PA: Holt, Rinehart and Winston)
[16] Willis R F and Christensen N E 1978 *Phys. Rev.* B **18** 5140
[17] Feydt J, Elbe A, Engelhard H, Meister G, Jung Ch and Goldman A 1998 *Phys. Rev.* B **58** 14007